STRUCTURAL AND MAGNETIC PROPERTIES OF Sr$_2$FeMoO$_6$ OBTAINED AT LOW TEMPERATURES

C. BARTHA[*], C. PLAPCIANU, A. CRISAN, M. ENCULESCU, A. LECA
National Institute of Materials Physics, 405A Atomistilor, 077125 Magurele-Ilfov, Romania

The double-perovskite Sr$_2$FeMoO$_6$ has been obtained by solid state method at low temperature (1060 °C) and a very short time of synthesis (up to 4h). Both, X-ray diffraction and scanning electron microscopy (SEM) confirmed the formation of Sr$_2$FeMoO$_6$ oxide with grain sizes around 160 mm, and a small amount of SrMoO$_4$ as an impurity. Mössbauer spectroscopy revealed a mixed site population with Fe and Mo ions generating a structure type with population inversion. This structure has a critical influence on the magnetic properties, as confirmed by the magnetization and T$_C$ values, i.e 3.56 μ$_B$ / f.u and 415 K, respectively. The Sr$_2$FeMoO$_6$ behavior was interpreted in terms of ferrimagnetic couplings generated by the various distributions of local interactions between Fe and Mo neighbors while comparing the ideal structure should show antiferromagnetic coupling between the two sublattices.

1. Introduction

The interest in Sr$_2$FeMoO$_6$ (SFMO) double perovskite oxide derives from both fundamental challenges and technological applications such as read/write heads, magnetic sensors, magnetic random access memory (MRAM) devices and spin injectors [1-3]. Sr2FeMoO6 has a cubic structure, where Fe and Mo atoms are inside an oxygen octahedron and the Sr atoms are positioned at the octahedral sites, in the center of the unit cell. However, in most of the cases, a B-site disorder or antisite (AS) disorder appears where the Fe is replaced by Mo and vice versa [4-6]. Depending of the Fe/Mo ordering and stoichiometry, SFMO has been reported to have either cubic Fm¯3m or tetragonal I$_4$/mmm structures [7]. Despite its apparent simplicity, this system shows several controversies related to the magnetic and electronic behavior. The ferrimagnetism of SFMO can be described as an ordered array of parallel Fe^{3+} (S=5/2) magnetic moments antiferomagnetically coupled with Mo^{5+} (S=1/2) spins. In this ideal arrangement, the saturation magnetization at low temperature would be 4 μ$_B$ / f.u. But, in real experiments, this value was never obtained, the highest magnetization obtained so far on SFMO polycrystalline was of 3.98 μ$_B$ / f.u. and a T$_c$ of 430 K [1, 8-9]. In the last years, many synthesis methods have been reported for SFMO, including the classic ones (solid state reactions, sol-gel, hydrothermal etc.) and the newest techniques such as spark plasma sintering or microwave synthesis [10-13]. The solid state method requires higher temperatures for calcination and sintering, as a prolonged dwell time, longer than in the wet-chemistry route. Since this material is very sensitive to air, the key element of the processing is to sinter SFMO precursors in a reducing atmosphere such as 5% H$_2$ / 95% Ar, in order to diminish the oxygen in excess and provide the appropriated stoichiometry. In this study, we present the results obtained on SFMO polycrystalline samples processed at low temperatures and short sintering times. Additionally, the influence of sintering parameters on SFMO structure and magnetic properties have been investigated.

---

[*]Corresponding author: cristina.bartha@infim.ro

2. Experimental

The synthesis of SFMO double perovskite was performed by solid state technique starting from $SrCO_3$ (Riedel-de Haën 97%), Fe_2O_3-red (Fluka > 97%) and MoO_3 (99.5% Reactivul Bucuresti) powders (2:0.5:1= $SrCO_3$:Fe_2O_3:MoO_3). The mixture has been homogenized in 96% ethanol using a Retsch PM 400 planetary mill, for 4 hours at 300 rpm to enhance the precursors reactivity and then dried in the oven for 2 hours at 70ºC to eliminate the ethanol. The SFMO precursors were heated in a Nabertherm muffle furnace at 900ºC for 4 hours, in the air, with 20ºC/min heating rate. Pellets having 20 mm in diameter were obtained from the calcined oxide powder, which were then sintered at 1060ºC in a quartz tube furnace for 4 hours using 5% H_2 / 95% Ar reducing atmosphere flow.

The SFMO samples were further investigated by thermogravimetric-differential scanning calorimetry (TG-DSC), X-ray diffraction, scanning electron microscopy (SEM), Mössbauer spectroscopy and magnetic properties analysis. The thermal investigation of the precursors was carried out from room temperature up to 1000°C with a SETARAM SETSYS Evolution18 instrument in TG-DSC Thermal Analyzer mode. Samples were measured in an open cylindrical alumina crucible, in synthetic air (80% N_2 / 20% O_2) at a standard heating rate of 10°C/min. using an empty alumina crucible as reference. X-ray diffraction was performed on a Bruker-AXS tip D8 ADVANCE diffractometer ($CuK_{\alpha 1}$ radiation) at room temperature with a step-scan interval 2θ of 0.02° and a step time of 10s. The crystallographic parameters and crystallite sizes were determined by quantitative phase analysis using Materials Analysis Using Diffraction (MAUD) software. The microstructure and the composition analysis (EDX) have been investigated by SEM, using a scanning electron microscope Evo 50 XVP with EDAX attachment (Carl Zeiss NTS). For Mössbauer spectra (MS) we used a constant acceleration spectrometer with symmetrical waveform and a 57Co (1.85 GBq) source. The measurements were performed at two different temperatures (5 K and 295 K) and the fitting spectra were carried out with the NORMOS program. The magnetization dependence of magnetic field was measured using a superconducting quantum interference device (SQUID) at three different temperatures (5, 150 and 295 K) in a magnetic field of 6 T. The Currie temperature, T_c, was determined by a PPMS Quantum Design device.

3. Results and discussions

3.1. Thermal analysis

The thermal analysis of SFMO precursors (Figure 1) reveals the existence of three distinct process stages. In the first stage, a small increase in mass ($\approx$ 3 %) was observed, which is due to the saturation of the surface vacancies with the oxygen atoms, followed by two steps up to 900°C. These processes are accompanied by two exothermic peaks on the DSC curve, centered at 619°C and 913°C, which correspond to a mass loss of $\approx$ 5% and $\approx$ 2% respectively. The first peak can be assigned to the thermal decomposition of the molybdenum anhydride) and the second one to strontium carbonate decomposition [14-15]. The last endothermic peak, centered around 968°C represents the temperature at which double perovskite structure begins to form [12]. Based on this information, the calcination temperature of the precursors was decided to be 900°C.
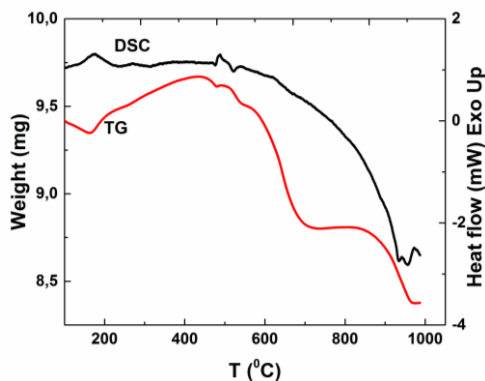
*Fig. 1 TG-DSC analysis of Sr₂FeMoO₆ precursors performed
in synthetic air (10°C/min. heating ramp rate).*

3.2. X-ray diffraction

The purity of phases in both calcined and sintered samples has been investigated by X-ray diffraction. Figure 2 shows the two diffractograms obtained on as calcined SFMO precursors in air (a) and after sintered treatment in 5% H_2 / 95% Ar atmosphere (b). The refinement of the crystal structure was performed by the Rietveld method.

X-ray powder analysis of the precursors treated in air shows the formation of a mixture of phases, where Sr_2FeMoO_6 is a majority, while $SrMoO_4$ was observed as an impurity . This structure is strongly improved during sintering, when the $SrMoO_4$ impurities are reduced considerably [16].
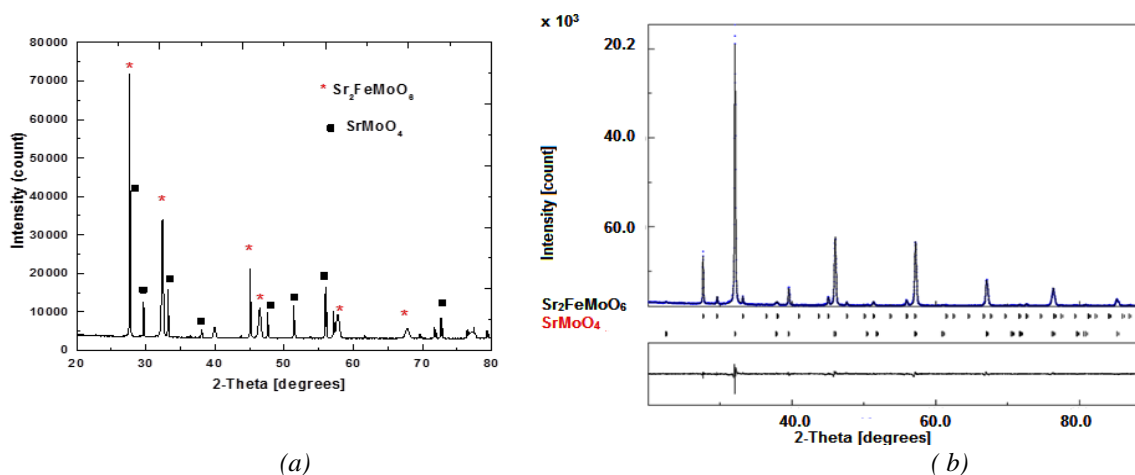

(a)   *(b)*

*Fig. 2 XRD diffraction performed on the Sr₂FeMoO₆ calcined in air (a) and Rietveld
profile of Sr₂FeMoO₆ sintered in 5% H / 95% Ar atmosphere (b).*

The Rietveld refinement was carried out based on a tetragonal structure with space group I_4/mmm and the resulted parameters are listed in Table 1.

*Table 1. The Rietveld refinement parameters of Sr₂FeMoO₆
sintered in 5% H / 95% Ar atmosphere.*

Phases	Weight (%)	Cell parameters (Å)	D (nm)
Sr_2FeMoO_6	96.66 +- 0.0	a = 5.5721 ± 0.0005 c = 7.9000 ± 0.0001	162
$SrMoO_4$	3.33 +- 0.3	a = 5.3979 ± 0.0001 c = 12.0600 ± 0.0006	316

The SFMO crystallite sizes are around 160 nm, comparable with those previously reported for samples prepared at higher temperatures and longer dwell time [17-19].

3.3. Scanning electron microscopy
The Figure. 3 shows the SEM images of SFMO samples: powder (a) and bulk (b).

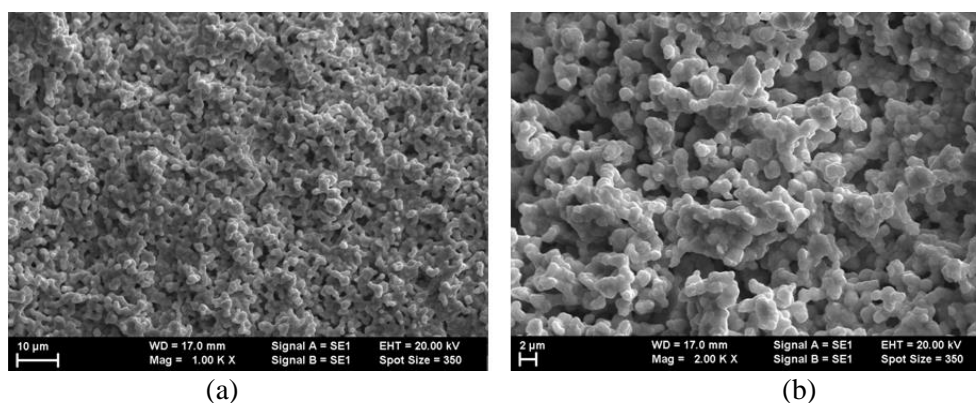(a)   (b)

Fig. 3 SEM images of Sr2FeMoO6 double-perovskite for powder (a) and bulk (b).

In both pictures, the particles appear uniform and their sizes are comparable with those determined by Rietveld analysis. The EDX spectrum presented in figure 4 confirms the presence of the constituent elements, i.e. Sr, Fe, Mo and O, the composition being nearly the same as the stoichiometric Sr_2FeMoO_6 (see table 2).
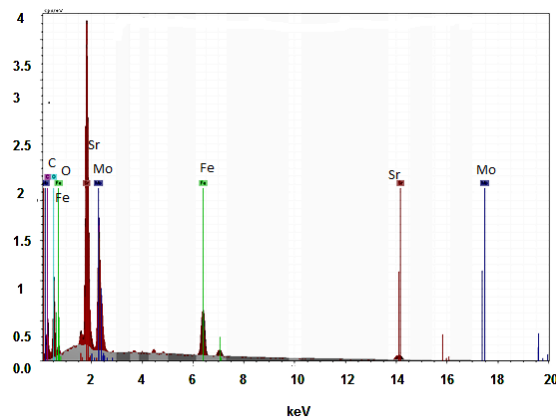

Fig. 4 EDX spectrum of Sr_2FeMoO_6 double-perovskite.

Table 2. Compositional analysis by EDX analysis of Sr_2FeMoO_6 double-perovskite

Element	Series	Mass (%)	Atom (%)	Error (%)
Strontium	L-series	42.50	20.36	1.8
Iron	K-series	10.04	7.55	0.3
Molybdenum	L-series	25.92	11.34	1.0
Oxygen	K-series	21.54	60.75	3.3
		100	100	

3.4. Mössbauer spectroscopy

Fig. 5 displays Mössbauer spectra (MS) acquired on the SFMO powders at two different temperatures, 10 K and 150 K respectively.
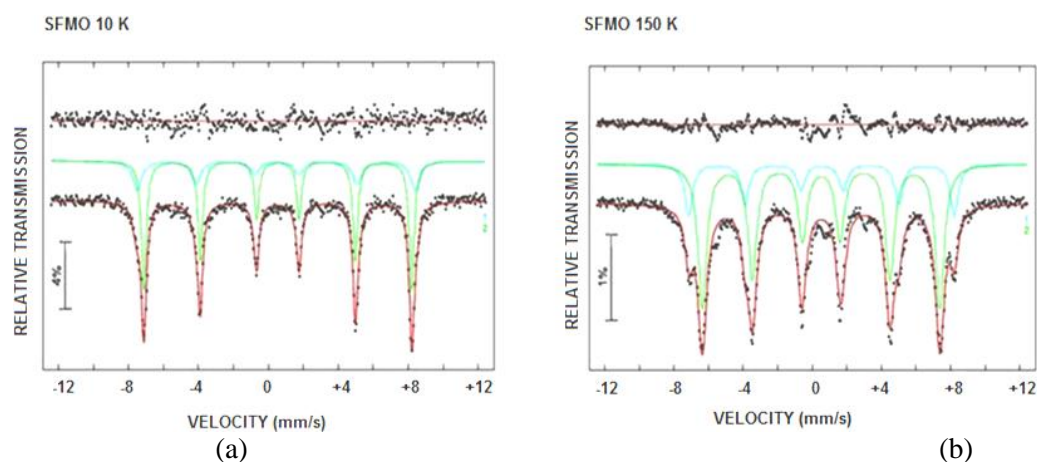

(a) (b)

Fig. 5 Mössbauer spectra of Sr_2FeMoO_6 acquired at two different temperatures:
10 K (a), respectively, 150 K (b)

The MS parameters of the two fits are listed below.

Table 3. Mössbauer parameters obtained from the two spectra: (B) –internal field at nucleus,
(IS)-isomer shift, (Γ)- line width and (A) is the relative area related to site population

Sample	B (T)	IS (mm/s)	Γ (mm/s)	A (%)
Sr_2FeMoO_6	49	0.455	0.627	29.69
10K	47	0.533	0.337	70.30
Sr_2FeMoO_6	47	0.541	0.544	22.02
150K	42	0.507	0.614	75.97

Both spectra consist mainly of a six-line absorption pattern, revealing the presence of magnetic order at these temperatures. The distance between lines offers relevant information about the internal magnetic field B, which is proportional to the magnetic moment of the iron. In both cases, MS spectra have been fitted with two crystalline networks, suggesting the presence of two positions for the Fe ions, one belonging to the B site and representing ca. 25%, while the rest being situated on the Mo (B') site. The sextet with B=49 T was assigned to Fe ions positioned on B site, while the sextet where B=47 T correspond to Fe ions positioned on B' site. Considering the fact that Fe hyperfine field is proportional to the spin density of 3d- electrons (in our case Fe ions), this case implies a lower value for an increased delocalization of the Mo electrons. The average of isomer shift is around 0.5 mm/s and represents a relatively high value for Fe^{3+} in the high spin state, suggesting a relative enhanced charge density at the Fe site [20-21].

3.5. Magnetic properties

The Currie temperature value T_c was determined from the magnetization versus temperature curve, M (T), at a magnetic field of 0.5 T (Fig.. 6).
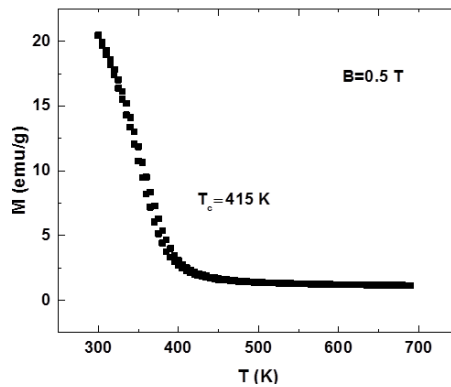
Fig. 6 M (T) curve obtained on Sr₂FeMoO₆ sample at a applied magnetic field of 0,5 T.

It has been found a T_c=415 K, which is similar with those values reported in literature for polycrystalline samples processed in special conditions [22-24]. The highest T_c value (T_c= 430 K) for SFMO type compound has been obtained for processing in a special condition, under high-pressure[1].

The M (H) curves obtained at three different temperatures: 5 K, 150 K and 295 K (Figure7) reveal a rapid increase of magnetization at low values of applied magnetic fields, induced by the magnetic moments alignment of Fe and Mo ions. In our case, the obtained T_c value demonstrated the fact that this compound can be processed in normal conditions (meaning low temperatures and short times of sintering) and it can be successfully used in various applications.
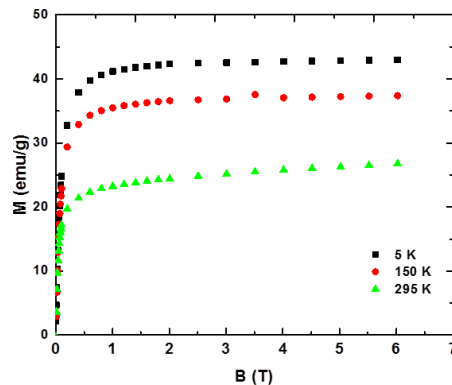

Fig. 7 Magnetization curves obtained at three different temperatures on Sr₂FeMoO₆ sample.

At high magnetic fields, the magnetic moments are already aligned and no difference between the three curves can be observed any longer. The magnetization at saturation of 3.56 µB/f.u is smaller than theoretical (4 µB/f.u) obtained for an ideal double perovskitic structure, in what case the Fe ions are found on the B site, while Mo ions occupy only the B' site . This value can be explained by the presence of both oxygen vacancies and Fe - Mo clusters in the SFMO oxide, which were generated by the mixed site occupation with the two ions, resulting a compound which is not in an ideal double-perovskite, but with an intermediate distribution structure. The electronic properties of SFMO oxide are strongly influenced by the cations' order in the crystal and the distribution of magnetic regions [25]. M(H) curves features can be easily understood taking into consideration the existence of two magnetic sublattices: one oriented parallel to the applied magnetic field and the second one having an antiparallel orientation to the applied magnetic field. In an ideal ordered SFMO structure, both FeO_6 and MoO_6 octahedra are alternating and form a ferromagnetic arrangement of O-Fe-Mo-O type [26]. We have demonstrated the existence of ferrimagnetic couplings generated by the existence of various Fe and Mo neighbors

coordination's which produce local interaction distributions. As a result, there is an antiferromagnetic coupling of the two sub-lattices, but with a ferrimagnetic result induced by the mono-element occupation [27-29].

4. Conclusions

Sr_2FeMoO_6 double-perovskite oxide has been processed at low temperature and very short time synthesis, generating a structure with a stoichiometry very close to the ideal one. Based on Mössbauer spectroscopy, which revealed the inverse occupation of both B, B' sites, notable effects and magnetic properties were interpreted in terms of the presence of mixed populations. Considering this model, the metal nearest neighbors are at the alternative site, and cluster areas around Fe ions with various sites occupied by Mo ions and/or Fe have been formed. The magnetic moment value of 3.56 μ_B / f.u is due to the occurrence of a ferrimagnetic distribution couplings arising from the presence of various of Fe and Mo neighbors where a local interactions distribution exist. It was also obtained a T_c value of 415 K, which is in good agreement with data reported until now for SFMO oxides synthesized by other methods which applied higher synthesis temperatures.

References

[1] M Retuerto, M J Martınez-Lope, M Garcıa-Hernandez, J A Alonso, J. Phys: Condens. Matter **21**, 186003 (2009).
[2] Y. Moritomo, S. Xu, A. Machida, T. Akimoto, E. Nishibori, M. Takata, M. Sakata, Phys. Rev. B **61**, R7827 (2000).
[3] C.W. Yang, T.T. Fang, J. Electrochem. Soc. **159**, 35 (2012).
[4] G. Aldica, C. Plapcianu, P. Badica, C. Valsangiacom, L. Stoica, J. of Magnetism and Magnetic Materials **311**, 665 (2007).
[5] C. Valsangiacom, C. Plapcianu, L. Stoica, G. Aldica, V. Kuncser, J. of Optoelectronics and Advanced Materials **10,** 4, 845 (2008).
[6] J. L. Alonso, L. A. Ferna´ndez, F. Guinea, F. Lesmes, and V. Martin-Mayor, Physical Review B **67**, 214423 (2003).
[7] G Y Liu, G H Rao, X M Feng, H F Yang, Z W Ouyang, W F Liu1 and J K Liang, J. Phys.: Condens. Matter **15,** 2053–2060 (2003).
[8] Kobayashi K I, Kimura T, Sawada H, Terakura K and Tokura Y , Nature, **395**, 677 (1998).
[9] J. Navarro, C. Frontera, D. Rubí, N. Mestres and J. Fontcuberta, Materials Research Bulletin **38**, 1477 (2003).
[10] M.X. Dai, C. Su, R. Wang, Z.L. Wang, Solid State Communications **119,** 377 (2001).
[11] M Cernea, F.Vasiliu, C. Bartha, C.Plapcianu, M. Mercioniu, Ceramics International, **40,** 8, 11601 Part: A (2014).
[12] M. Cernea, F. Vasiliu, C. Plapcianu, C.Bartha, I. Mercioniu, I. Pasuk, R. Lowndes, R. Trusca, G. V. Aldica, L. Pintilie, J. Eur. Ceram. Soc. **33**(13-14), 2483 (2013).
[13] Yong-Qing Zhai, Jing Qiao, and Man-De Qiu, E-Journal of Chemistry **9**(2), 818 (2012).
[14] J. B. B.Heynes, , J. J Cruywagen Inorganic Syntheses **24**, 191 (1986).
[15] S. Maitra , N. Chakrabarty , J. Pramanik, Cerâmica, **54**, 268 (2008).
[16] A. Dinia, J. Vénuat, S. Colis, G. Pourroy, Catalysis Today, **89**, 297 (2004).
[17] Y. C. Hu, J. J. Ge, Q. Ji, B. Lv, G. F. Cheng, X. S. Wua, Powder Diffr.Suppl. **25**, S1 (2010).
[18] Jibu Stephen , Materials Science Forum Vol. **700**, 19 (2012).

[19] D D Sarma and Sugata Ray, Proc. Indian Acad. Sci. (Chem. Sci.) **113**(5-6), 515 (2001).

[20] P.A Algarabela, L Morellona, J.M De Teresaa, J Blascoa, J Garcíaa, M.R Ibarraa,
    T Hernándezb, F Plazaolab, J.M Barandiaránb, Journal of Magnetism and Magnetic Materials,
    226-230, 1098 (2001).

[21] M. Raekers, K. Kuepper, H. Hesse, I. Balasz, I.G. Deac, S. Constantinescu, E. Burzo,
    M. Valeanu, M. Neumann, Journal of Optoelectronics and Advance Materials,
    8(2), 455 (2006).

[22] N E Brese, M. O'Keefe , Acta Crystallogr. B **47**, 192 (1991).

[23] R P Borges, R M Thomas, C Cullinan, J M D Coey, R Surynarayanan, L Ben-Dor,
    L P Gaudart, A Revcolevski, Condens. Matter **L445–L450** (1999).

[24] C. Ritter, J. Blasco, J.-M. De Teresa, D. Serrate, L. Morellon, J. Garcia, M. R. Ibarra,
    Solid St. Science **6,** 419 (2004).

[25] M. Garcia-Hernandez, J.L. Martinez, M. J. Martinez-Lopez, M. T. Casaris, J.A. Alonso, Phys.
    Rev. Lett. **86**, 2443 (2001).

[26] Z. Szotek, W. M. Temmerman, A. Svane, L. Petit, G.M. Stocks, H. Winter, Journal of
    Magnetism and Magnetic Materials, **272-276**, 1816-1817 (2004).

[27] B. Jurca, J. Berthon, N. Dragoe, P. Berthet, Journal of Alloys and Compounds,
    474, 416 (2009).

[28] M. Chung, P.J. Huang, W-H. Li, C.C. Yang, T.S. Chan, R.S. Liu, S.Y. Wu, J.W. Lynn,
    Physica B **385-386**, 418 (2006).

[29] R. Allub, O. Navarro, M. Avignon, B. Alascio, ¸Physica B **13-17** (2002).